iScience

CellPress
OPEN ACCESS

Article

Ganoderma lucidum extract attenuates corticotropin-releasing hormone-induced cellular senescence in human hair follicle cells

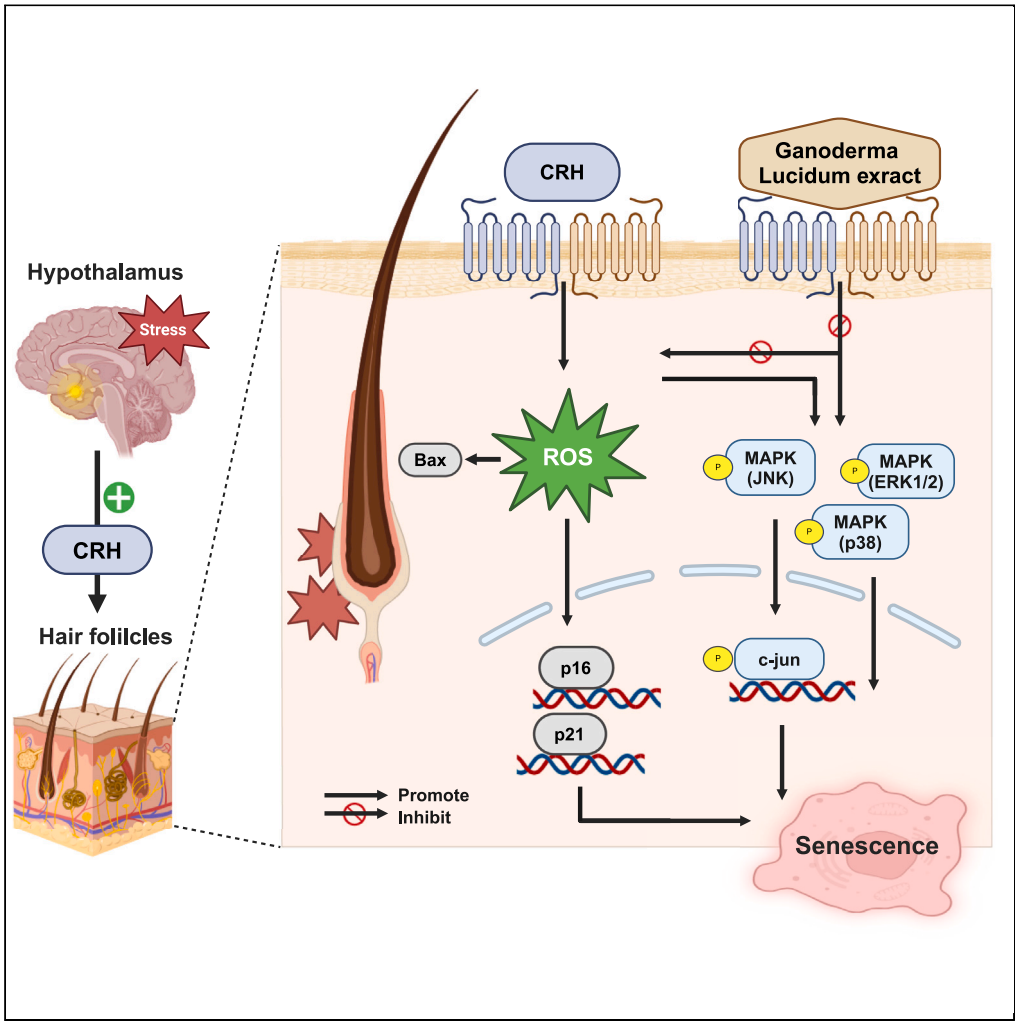

Sunhyoung Lee, So Young Kim, Seunghee Lee, ..., Youngji Kwon, Jaehwan Choi, Ohsang Kwon

oskwon@snu.ac.kr

Highlights

CRH led to stress-induced senescence in human hair follicle cells

GL extract attenuated stress-induced hair follicular senescence

GL extract could delay catagen entry and scavenge ROS

GL extract can be used for treating stress-induced hair loss

Lee et al., iScience *27*, 109675
May 17, 2024
https://doi.org/10.1016/j.isci.2024.109675

iScience

CellPress
OPEN ACCESS

Article

Ganoderma lucidum extract attenuates corticotropin-releasing hormone-induced cellular senescence in human hair follicle cells

Sunhyoung Lee,[1,2,5] So Young Kim,[1,5] Seunghee Lee,[1,2] Sunhyae Jang,[1] Sungjoo Tommy Hwang,[3] Youngji Kwon,[4] Jaehwan Choi,[4] and Ohsang Kwon[1,2,6,*]

SUMMARY

Corticotropin-releasing hormone (CRH) is a key mediator in stress-induced hair growth inhibition. Here, we investigated the impact of stress-induced senescence and evaluated the potential of *Ganoderma lucidum* (GL) extract in mitigating CRH-induced senescence in human hair follicle cells (hHFCs). We show that CRH treatment increased the senescence-associated beta-galactosidase (SA-β-GAL) activity and reactive oxygen species (ROS) formation in hHFCs and suppressed alkaline phosphatase (ALP) activity and anagen-inducing genes. However, GL extract restored ALP activity and decreased the expression levels of anagen-related genes in CRH-treated hHFCs. It decreased SA-β-GAL activity, reduced ROS production, and prevented the phosphorylation of MAPK signaling pathways in CRH-related stress response. Moreover, GL reversed the CRH-induced inhibition of two-cell assemblage (TCA) elongation and Ki67 expression. GL extract attenuates stress-induced hair follicular senescence by delaying catagen entry and scavenging ROS. Our findings suggest that GL extract could be used for treating stress-induced hair loss.

INTRODUCTION

Hair follicles are skin appendages consisting of mesenchyme-derived dermal papilla cells (DPCs) and epithelium-derived outer root sheath cells (ORSCs).[1] They undergo distinct cyclic stages of hair growth (anagen), regression (catagen), and rest (telogen).[2] Hair follicle miniaturization, closely associated with aging, results in hair thinning, weakening, and shrinking, ultimately leading to hair loss.[3] The primary events in hair follicle aging involve a decrease in the number of hair follicle stem cells and an accelerated hair cycling process, contributing to hair loss.[3] Sudden or gradual hair loss, known as alopecia, has increased among both men and women, and is predominantly attributed to environmental stressors such as an unhealthy diet, stress, drugs, smoking, skin issues, and hormonal imbalances rather than genetic factors. Consequently, it has become a growing concern worldwide.[4]

During exposure to stressful events, catecholamines such as epinephrine, norepinephrine, and dopamine are secreted from the adrenal medulla and sympathetic nervous system.[5] Additionally, following exposure to environmental stressors, the hypothalamic-pituitary-adrenal (HPA) axis is activated and corticotropin-releasing hormone (CRH) is sequentially released from the hypothalamus.[6] CRH stimulates adrenocorticotropic hormone (ACTH) secretion from the anterior pituitary gland, which subsequently triggers the release of corticosteroids from the adrenal cortex.[5] This hormonal stress response is regulated by various stress hormones, including CRH, ACTH, and glucocorticoids (GCs), all of which play crucial roles in target organs.[7]

The skin serves as a target organ for neuroendocrine signals, with CRH and proopiomelanocortin (POMC) signaling pathways regulating the stress response of the skin.[8–10] The skin and hair follicle are extensively innervated with sensory and autonomic nerve fibers and play crucial roles in maintaining stress-related homeostasis.[8–10] The neurohormones, neurotransmitters, and cytokines released in response are involved in a complex interplay at various stages of the hair growth cycle and significantly impact it.[11–13] A local HPA axis is also activated in the skin exposed to environmental stress.[14] The HPA axis is a crucial neuroendocrine system that acts as a coordinator and organizer of local response to stress that may function as a cutaneous defense system with all components of the HPA axis expressed in the skin.[10,15,16] The secretable components of the HPA axis expressed in dermal fibroblast, which respond to CRH by activating cyclic adenosine monophosphate,

[1]Department of Dermatology, Seoul National University College of Medicine, Laboratory of Cutaneous Aging and Hair Research, Biomedical Research Institute, Seoul National University Hospital, Institute of Human-Environment Interface Biology, Medical Research Center, Seoul National University, Seoul 03080, South Korea
[2]Department of Biomedical Sciences, Seoul National University College of Medicine, Seoul 03080, South Korea
[3]Dr. Hwang's Hair-Hair Clinic, Seoul 06035, South Korea
[4]R&I Center, COSMAX BTI, Seongnam, Gyeonggi-do, South Korea
[5]These authors contributed equally
[6]Lead contact
*Correspondence: oskwon@snu.ac.kr
https://doi.org/10.1016/j.isci.2024.109675

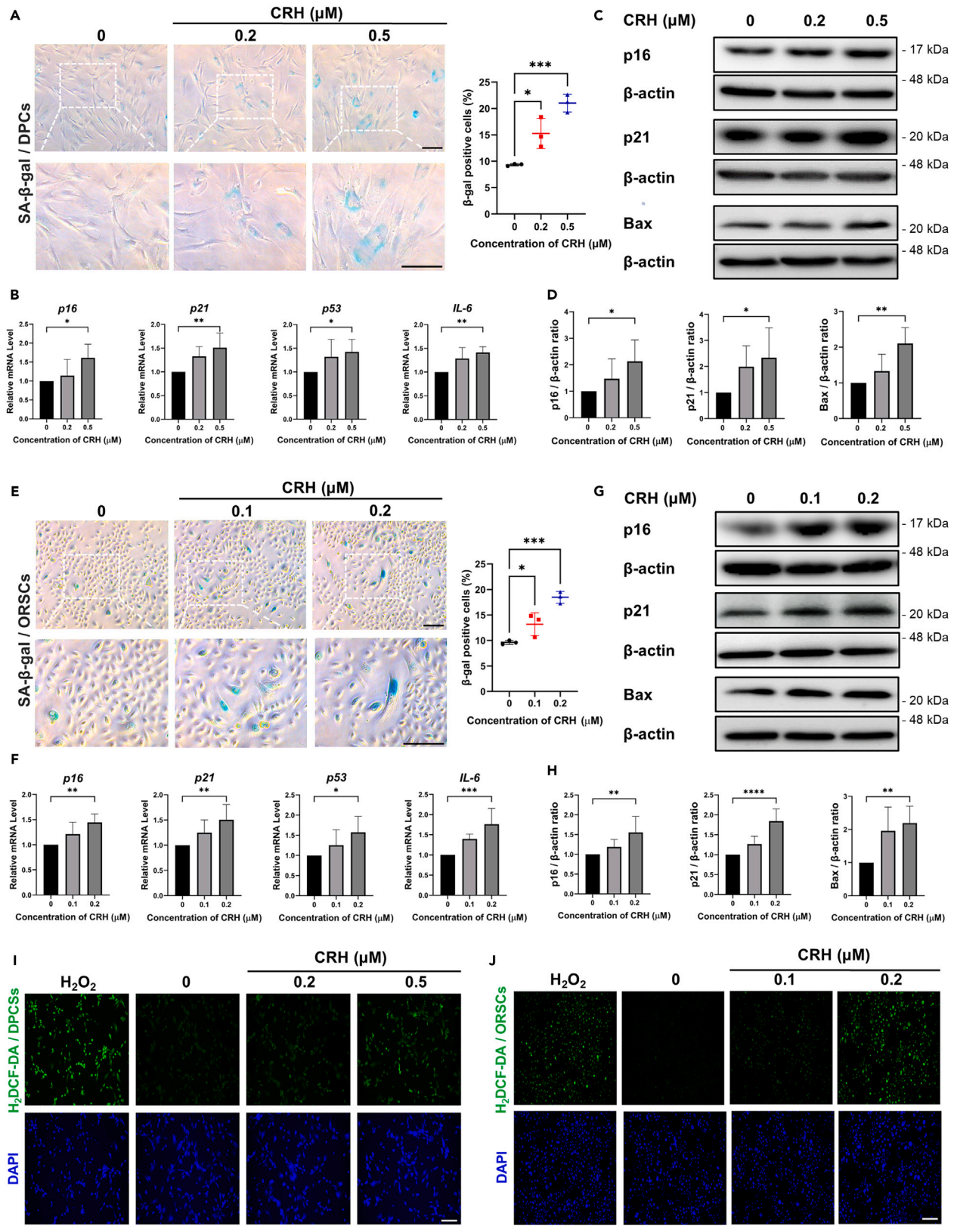
A
CRH (μM)
0
0.2
0.5
SA-β-gal / DPCs
β-gal positive cells (%)
Concentration of CRH (μM)
C
CRH (μM)
p16
β-actin
p21
Bax
17 kDa
48 kDa
20 kDa
B
p16
p21
p53
IL-6
Relative mRNA Level
D
p16 / β-actin ratio
p21 / β-actin ratio
Bax / β-actin ratio
E
SA-β-gal / ORSCs
0.1
G
F
H
I
J
H2O2
H2DCF-DA / DPCSs
H2DCF-DA / ORSCs
DAPI

Figure 1. Effects of corticotropin-releasing hormone (CRH) on cellular senescence and reactive oxygen species (ROS) generation in human hair follicle cells (hHFCs)

(A, B, C, D, I) Dermal papilla cells (DPCs) and (E, F, G, H, J) outer root sheath cells (ORSCs). The DPCS and ORSCs were treated with 0.2–0.5 μM and 0.1–0.2 μM CRH, respectively, for 48 h.

(A, E) Premature senescence of hHFCs induced by CRH. Senescence-associated β-galactosidase (SA-β-GAL) activity after CRH treatment was determined using the SA-β-GAL assay. The graphs depict mean ± SD values from three independent experiments. SA-β-GAL-positive cells were imaged using a microscope.

(B, F) RT-qPCR analysis was performed to assess the expression of *p16*, *p21*, *p53*, and *IL-6* mRNA following CRH treatment. The graphs show the quantification results, indicating mean ± SD values from five independent experiments.

(C, G) Cultured cells were lysed, and western blotting was performed to detect p16, p21, and Bax protein expression.

(D, H) Protein levels were quantified through densitometric analysis. Data are represented as mean ± SD values from five independent experiments.

(I, J) Reactive oxygen species (ROS) formation at the cell level was measured using 2,7-dichlorodihydrofluorescein diacetate (H_2DCF-DA). Hydrogen peroxide (H_2O_2; 200 μM) was used as a positive control. Nuclei were stained with 4′,6-diamidino-2-phenylindole (DAPI). CRH treatment resulted in H_2DCF-DA-positive fluorescence signals in the cultured cells (blue: DAPI; green: H_2DCF-DA). Fluorescence was detected using a fluorescence microscope and a microplate reader (Figure S3). Scale bar, 100 μm Data represent the mean ± SD. Statistical significance was calculated using one-way analysis of variance with Dunnett's multiple comparisons test. *$p < 0.05$, **$p < 0.01$, ****$p < 0.0001$.

expressing the POMC gene and protein, and producing ACTH.[16,17] However, the cutaneous HPA axis shows differential susceptibility to ultraviolet radiation.[15]

CRH (previously known as a corticotrophin-releasing factor), a proximal component of the HPA axis, is a 41-amino acid peptide that plays a pivotal role in the neuroendocrine response to stress.[18] Several studies have demonstrated that CRH and its receptors are extensively distributed in hair follicles.[18–20] CRH family members bind to two receptor types: CRHR1 and CRHR2. CRHR1 exhibits high expression levels in the hair matrix area,[18,21] while both receptors have been detected in human DPCs.[19] Corticotropin-releasing hormone receptor and melanocortin-1 receptor are expressed in the follicular epithelium and mesenchyme during hair growth in both mice and humans.[22,23] Specifically, CRH and CRH receptors are differentially expressed in mammalian skin.[17,24,25] In addition, the intracutaneous concentration of the CRH and expression of CRHR1 exhibit similar cyclic changes, aligned with the hair cycle in the skin of C57BL/6 mice, with the highest levels noted in the anagen phase and lowest levels in the catagen and telogen phase.[22] Numerous studies have investigated the interactions between stress hormones and hair loss.[25,26] Alterations in the CRH system and chronically elevated CRH levels are implicated in stress-related hair loss, primarily inducing catagen, inhibiting cell proliferation,[17,19] and triggering mast cell degranulation.[27] Consequently, CRH has been identified as a key mediator in stress-induced hair growth inhibition.[18] However, the exact role of CRH in hair growth inhibition remains unknown.

Ganoderma lucidum (GL) is a red-colored species within the *Ganoderma* genus, classified under the Ganodermataceae family. It is a Chinese traditional medicinal mushroom and is widely distributed in Asian countries. GL extracts have been reported to provide protection against various disorders, including chronic bronchitis, bronchial asthma, diabetes, and cancer.[28] The primary bioactive components of GL extracts include abundant polysaccharides and triterpenoids such as lucidenic and ganoderic acids, which exhibit potent biological activities, including antibacterial, antioxidant, anti-aging, and anti-inflammatory effects.[29–32] GL triterpenoid fractions possess immunomodulatory properties with anti-radiation, anti-tumor, and antioxidant effects.[28] Furthermore, GL polysaccharide fractions have been shown to prevent oxidative stress in murine skeletal muscle and extend lifespan through their antioxidant effects on aging skin cells.[33,34] Moreover, ganoderic acid, one of the main triterpenoids in GL, exhibits anti-inflammatory, immune-stimulatory, antioxidant, anti-aging, and anti-platelet aggregation effects.[31,32] Nevertheless, the effects of the GL extract on stress-induced human hair follicle senescence are unknown.

The objective of this study was to evaluate stress-induced follicular senescence in human hair follicle cells (hHFCs) and investigate whether the restorative effects of GL extract on stress-induced hair growth inhibition are functional in hHFCs and the two-cell assemblage (TCA) system. Through these investigations, we aimed to elucidate the mechanisms underlying cellular recovery mediated by GL extract in stress-induced human hair follicular aging.

RESULTS

Corticotropin-releasing hormone induces premature senescence and alters gene expression

Previously, we reported that glucocorticoid inhibits the growth of human DPCs.[25] In this study, we investigated the effects of CRH on the viability of human hair follicular cells, specifically DPCs and ORSCs. We exposed these cells to various concentrations of CRH and assessed cell viability using a Cell Counting Kit-8 (CCK-8) assay. As shown in Figures S1A and S1B, in the presence of 1 μM CRH, the viability of DPCs decreased compared with that in the control group. However, CRH concentrations of 0.1–0.5 μM and 0.1–0.2 μM did not induce cytotoxicity in DPCs and ORSCs, respectively. Therefore, these concentration ranges were selected for subsequent analyses.

To determine whether CRH induces cellular senescence in hair follicular cells, we exposed DPCs and ORSCs to various CRH concentrations for 48 h and assessed cellular senescence through a senescence-associated beta-galactosidase (SA-β-GAL) staining assay. The number of SA-β-GAL-positive cells increased following treatment with CRH (Figures 1A and 1E). Quantitative analysis of SA-β-GAL activity revealed an increase in the percentage of SA-β-GAL-positive cells in both cell types. Additionally, we performed real-time quantitative reverse transcription PCR (RT-qPCR) analysis to evaluate the expression levels of senescence-related genes, including *p16, 21, p53*, and interleukin-6 (*IL-6*). As shown in Figures 1B and 1F, CRH treatment significantly upregulated the expression of these genes in both cell types compared with that in untreated cells. Moreover, CRH treatment led to an increased expression of p16, p21, and Bax, a pro-apoptotic protein (Figures 1C, 1D, 1G, and 1H). These findings suggest that CRH plays a role in premature cellular senescence and stimulates apoptotic pathways in hair follicle cells.

Corticotropin-releasing hormone induces reactive oxygen species production

ROS are byproducts of oxidative stress and have been associated with DNA damage and cellular membrane dysfunction. Elevated ROS levels are a key factor in the aging process, mediating the interplay between redox signaling and oxidative stress.[35] Premature cellular senescence is closely linked to ROS production induced by stress hormones.[18] Therefore, we evaluated intrinsic ROS generation in both cell types in response to CRH. ROS production was measured using 2′,7′-dichlorodihydrofluorenscein diacetate (H_2DCF-DA) fluorescence staining. Fluorescence imaging revealed that CRH-treated cells exhibited higher fluorescence intensity than untreated cells (Figures 1I and 1J), similar to the fluorescence observed after treatment with 200 μM H_2O_2 (positive control). Quantitative analysis of H_2DCF-DA intensity using a spectrophotometer also revealed a significant increase in ROS levels in both cell types compared with that in the H_2O_2-treated cells (Figures S3A and S3B). The CRH group exhibited higher fluorescence intensities in both cell types compared with that in the H_2O_2 group, indicating that CRH increases ROS production in hair follicle cells.

Corticotropin-releasing hormone decreases the expression of hair growth factors and the axis length of two-cell assemblage

We investigated the effects of CRH on hair growth by applying it to both a monolayer (2D) and a 3D co-culture system referred to as the TCA *ex vivo* system. In a previous research, we demonstrated that this polar elongated structure co-culture system, composed of two types of hHFCs, enables the specific examination of the hair growth-modulatory effects of candidate substances.[36] We confirmed the aggregation of two types of hair follicle cells, DPCs and ORSCs, forming a TCA structure. Subsequently, we exposed the TCA to various concentrations of CRH for 5 days. A CRH concentration of 0.5 μM significantly suppressed TCA elongation (Figures 2A and 2B), indicating that CRH inhibits hair growth in hair follicular cells.

Furthermore, to determine whether CRH downregulates the expression of dermal papilla signature genes, we analyzed the expression levels of anagen-related genes and growth factors using qPCR. The results revealed a significant downregulation of various genes, including fibroblast growth factor (*FGF*) 7, *FGF10*, platelet-derived growth factor alpha (*PDGFA*), platelet-derived growth factor receptor beta (*PDGFR-β*), vascular endothelial growth factor (*VEGF*), alkaline phosphatase (*ALP*), and versican, upon treatment with CRH (0.5 μM) for 48 h (Figure 2C). Additionally, we measured ALP enzyme activity using an ALP staining assay, which showed a significant decrease in ALP enzyme activity following 0.5 μM CRH treatment for 48 h (Figure S4). These findings confirm that CRH-induced signals released from DPCs potentially lead to the suppression of hair follicle growth.

GL extract increases the TCA elongation and secretion of growth factors

In the GL extract-treated group, a significant increase in TCA length was observed compared with that in the control group (Figures 3A and 3B). Based on these findings, we hypothesized that the GL extract regulates and enhances the proliferation of ORSCs by releasing various growth factors from DPCs. For investigating this hypothesis, DPCs were treated with 20 μg/mL GL extract, and a human growth factor array was used to assess the levels of the evaluated growth factors. In the conditioned medium of DPCs, the signal intensities of insulin-like growth factor binding protein (IGFBP)-2, IGFBP-6, insulin-like growth factor (IGF)-1, IGF-1R, vascular endothelial growth factor (VEGF)-A, platelet-derived growth factor (PDGF) receptor β and PDGF-AA were significantly increased (Figure 3C).

Ganoderma lucidum extract attenuates corticotropin-releasing hormone-induced senescence and reactive oxygen species production in hair follicle cells

We investigated the effect of the GL extract on CRH-induced senescence of hair follicular cells. To examine the anti-senescence effect of the GL extract on CRH-treated cells, we used the SA-β-GAL assay and measured the mRNA expression of senescence-associated genes. Our results indicated a significant reduction in the percentage of SA-β-GAL-positive cells in DPCs and ORSCs following GL extract treatment (Figures 4A and 4E). Quantitative analysis of SA-β-GAL activity in cells treated with GL extract showed that the percentage of SA-β-GAL-positive cells was decreased in both cell types. Additionally, GL treatment resulted in decreased mRNA levels of senescence-associated genes, including *p16*, *p21*, *p53*, and *IL-6*, compared with those in the control group (Figures 4B and 4F). Consistent with these gene expression findings, the protein levels of p16, p21, and Bax, a pro-apoptotic protein associated with the catagen phase of the hair cycle, indicated that the GL extract attenuates cellular senescence (Figures 4C, 4D, 4G, and 4H). To further investigate the ROS-scavenging effects of the GL extract, H_2DCF-DA staining was performed on CRH-treated cells. H_2DCF-DA staining showed that treatment with the GL extract decreased CRH-induced ROS levels (Figures 4I and 4J). The H_2DCF-DA fluorescence intensity also indicated higher levels of CRH-induced ROS in both cell types treated with the GL extract (Figures S5A and S5D). Furthermore, we performed flow cytometry analysis to measure the H_2DCF-DA intensity in both cell types. Consistent with the results of the microplate assay, we observed that the increase in CRH-induced ROS levels, similar to that in H_2O_2 treatment, was reduced by the GL extract treatment (Figures S5B, S5C, S5E, and S5F). Moreover, the GL extract treatment resulted in a significant decrease in general cellular ROS levels.

Ganoderma lucidum extract restores the corticotropin-releasing hormone-induced suppression of growth factors and two-cell assemblage elongation

We observed a significant reduction in TCA length in the CRH treatment group compared with that in the control group. Therefore, we examined whether the GL extract restores the CRH-induced suppression of TCA length. In the CRH treatment group, we observed a clear

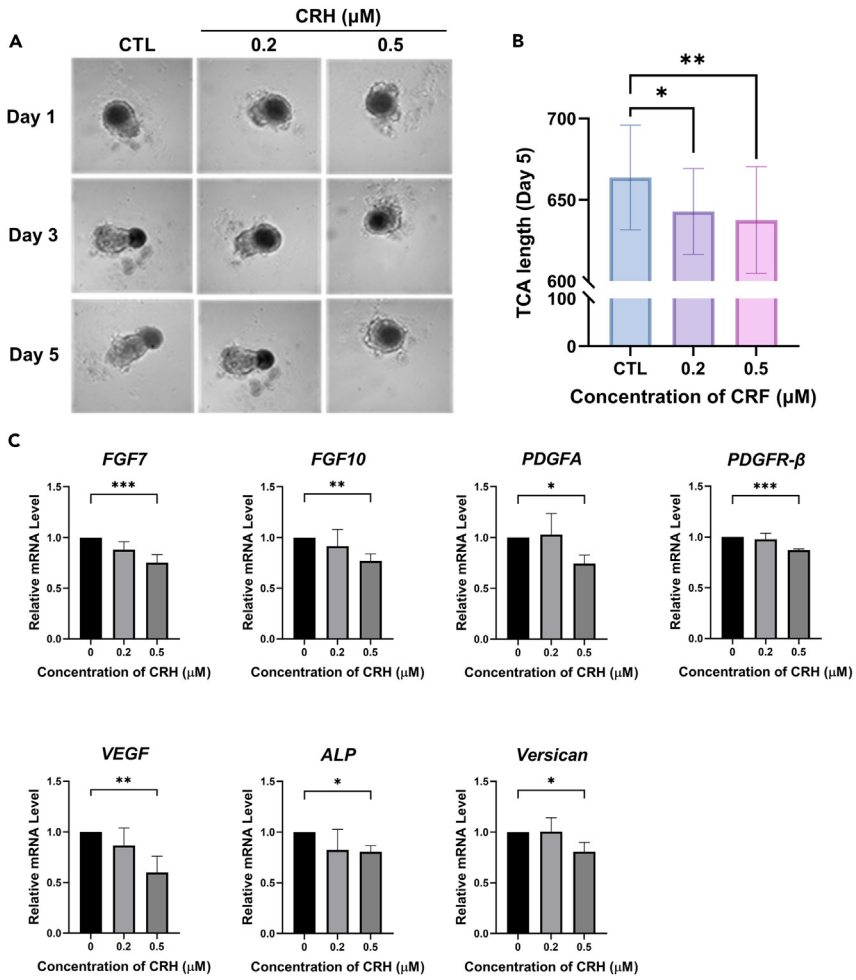

Figure 2. Effects of corticotropin-releasing hormone (CRH) on two-cell assemblage (TCA) elongation and hair growth-related gene expression

The TCAs were treated with CRH (0.2–0.5 μM) for 5 days.

(A) Representative images and (B) graph of TCA length measured using high-content screening (HCS). CRH significantly reduced the TCA elongation compared with that in the control. The graph presents quantification results. The dermal papilla cells (DPCs) were treated with CRH (0.2–0.5 μM) for 48 h. (C) RT-qPCR analysis was performed to evaluate the expression of *FGF7*, *FGF10*, *PDGFA*, *PDGFR-β*, *VEGF*, *versican*, and *ALP* mRNAs after CRH treatment. ALP enzyme activity was analyzed by ALP staining (Figure S4). The graphs show the quantification results. Data are represented as mean ± SD of five independent experiments. Statistical significance was calculated using one-way analysis of variance with Dunnett's multiple comparisons test. *$p < 0.05$, **$p < 0.01$, ***$p < 0.001$.

recovery of TCA elongation in the presence of the GL extract compared with that in each group treated with CRH-alone (Figures 5A and 5B).

To determine whether the GL extract restored the levels of CRH-inhibited growth factors, we examined the expression levels of several growth factors and ALP enzyme activity. The expression levels of anagen-related genes and growth factors, such as, *FGF7*, *FGF10*, *PDGFA*, *PDGFR-β*, *VEGF*, *ALP*, and *versican*, which were downregulated by CRH, were effectively recovered by the GL extract treatment (Figure 5C). The ALP enzyme activity of DPCs in the CRH treatment group, in the presence of the GL extract, was substantially rescued (Figure S6A).

To confirm the effect of the GL extract on hair growth, hair follicles were treated with the GL extract in the presence of CRH, and the number of Ki67-labeled cells was quantified through immunofluorescence staining. As shown in Figure S6B, the number of cells that were positive for Ki67, which is a marker for cell proliferation, decreased significantly following CRH treatment. This decrease was reversed after treatment with the GL extract.

Ganoderma lucidum extract attenuates the phosphorylation of mitogen-activated protein kinase signaling pathways in corticotropin-releasing hormone-induced stress response

Based on the results regarding the effectiveness of the GL extract in preventing CRH-induced cellular senescence and growth inhibition in DPCs and ORSCs, we sought to elucidate the underlying mechanism responsible for these effects. The roles of the mitogen-activated protein

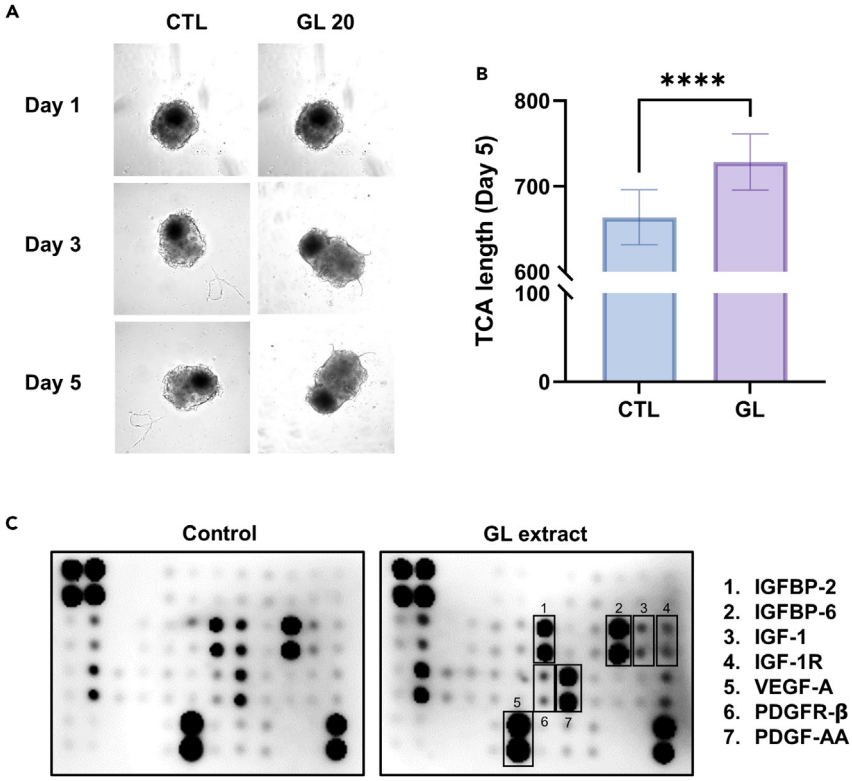

Figure 3. Effect of *Ganoderma lucidum* (GL) extract on two-cell assemblage (TCA) elongation and the secretion of growth factors in human dermal papilla cells

The TCA was treated with GL extract (20 μg/mL) for 5 days.

(A) Representative images and (B) graph showing TCA length measured using high-content screening (HCS).

(C) The secretion of growth factor in the medium containing GL extract from DPCs was assessed using a human growth factor antibody array, which analyzed 41 growth factors. Data are presented as the mean ± SD of three independent experiments. Statistical significance was calculated using one-way analysis of variance with unpaired *t*-test. ****$p < 0.0001$.

kinase (MAPK) pathway in mediating the effects of CRH have been reported.[37] To investigate this, the cells were treated with CRH alone or in combination with the GL extract, and the levels of *p*-JNK, p-*c*-jun, *p*-Erk1/2 and p-p38 were determined through western blot analysis. The results indicated that CRH upregulated the phosphorylation of JNK, c-jun, Erk1/2, and p38, thereby, activating cellular stress responses such as oxidative stress. Conversely, GL treatment reduced the phosphorylation of MAPK pathways in the CRH-treated cells, indicating the inactivation of stress-induced responses (Figures 6A and 6B). These findings suggest that the GL extract has an inhibitory effect on the CRH-induced activation of MAPK pathways.

DISCUSSION

GL extract is a natural biomaterial with various medicinal effects; for example, it reduces oxidative stress and exhibits anti-senescence properties.[29,30,38] However, the specific anti-senescence effects of GL extract on stress responses in hHFCs remain poorly understood, and its impact on CRH-induced SA-β-GAL activities and senescence-related marker expression has not been previously reported. In this study, we investigated the preventive effect of the GL extract on follicular senescence induced by CRH-associated stress responses in hHFCs and a TCA system.

Emerging research has highlighted the crucial role of stress-induced cellular senescence in the anagen-to-catagen hair cycle transition, which ultimately leads to hair loss.[18] Local stress response factors, such as CRH, propiomelanocortine peptides, glucocorticoid hormones, and autonomic neurotransmitters, are involved in stress-associated hair growth inhibition.[39] In a previous study, we demonstrated that GCs, which are stress hormones, inhibit cell proliferation, the expression of hair growth factors such as VEGF and HGF, and induce cell-cycle arrest in human DPCs.[25] Other studies have also identified GCs as potent hair growth suppressors that accelerate catagen entry and induce hair growth in murine hair follicles.[40,41] CRH stimulates the secretion of inflammatory cytokines such as TNF-α and IL-6 in neural cells,[42] and a CRHR1 antagonist has been shown to protect against the upregulation of inflammatory cytokines in stress-related responses.[43] Additionally, CRH induces the secretion of cortisol through ACTH in human hair follicles (anagen VI), leading to the induction of the catagen cycle, apoptosis of hair follicular keratinocytes, and high expression in the hair matrix area.[18] Recent studies have also revealed that CRH accelerates

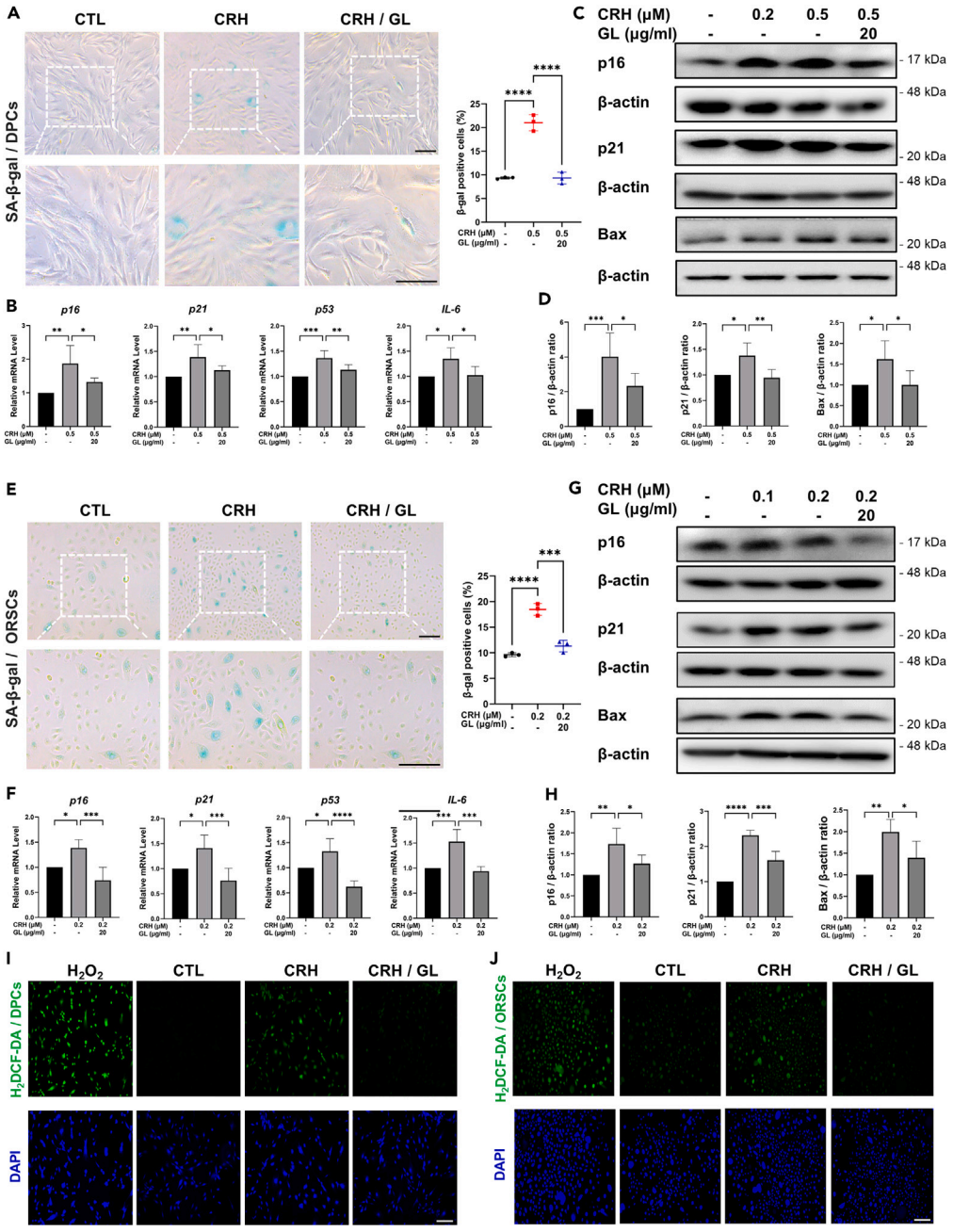

Figure 4. *Ganoderma lucidum* (GL) extract treatment attenuates the premature stress-induced hair follicle senescence effects of corticotropin-releasing hormone (CRH)

(A, B, C, D, I) DPCs and (E, F, G, H, J) ORSCs were treated with 0.2–0.5 μM and 0.1–0.2 μM CRH, respectively, in the absence and presence of GL extract (20 μg/mL) for 48 h.

(A, E) Senescence-associated beta-galactosidase (SA-β-GAL) activities of the DPCs and ORSCs treated with CRH in combination with GL extract were measured using the SA-β-GAL assay. The graphs show the quantification results. Graphs represent the mean ± SD values from three independent experiments. SA-β-GAL-positive cells were detected using a microscope.

(B, F) Cultured cells were lysed and RT-qPCR analysis was performed to determine the expression of *p16*, *p21*, *p53*, and *IL-6* mRNA. The graphs show the quantification results. Graphs represent the mean ± SD values from five independent experiments.

(C, G) Expression of p16, p21, and Bax protein was determined using western blotting. Equal protein loading was confirmed based on β-actin levels.

(D, H) The graphs present a quantitative representation of the reduction in the levels of p16, p21, and Bax following CRH treatment in the absence or presence of GL extract. Graphs show mean ± SD values from five independent experiments.

Figure 4. *Continued*

(I, J) The DPCs and ORSCs were incubated with 0.5 and 0.2 μM CRH, respectively, or 200 μM H_2O_2 (control), with GL extract (20 μg/mL). ROS formation at the cell level was assessed using H_2DCFDA. Cell nuclei were stained with DAPI. Fluorescence signals were determined using a fluorescence microscope, a microplate reader (Figures S5A and S5B) and a flow cytometry analysis (Figures S5B, S5C, S5E, and S5F). Scale bar, 100 μm Data are presented as mean ± SD. Statistical significance was calculated using one-way analysis of variance with Tukey's multiple comparisons test. *$p < 0.05$, **$p < 0.01$, ***$p < 0.001$, ****$p < 0.0001$.

anagen–catagen transition in human hair follicles by increasing the levels of transforming growth factor β2 (TGF-β2), inhibiting matrix cell proliferation, and suppressing insulin-like-growth factor-1 (IGF-1) levels.[19]

In this study, CRH significantly reduced the number of Ki67-positive cells in human hair follicle (HF) organ culture, and promoted the catagen transition of human HFs *in vitro*. These findings align with those of previous reports on stress-induced catagen transitions.[18]

Stress signals trigger the release of stress hormones from the adrenal gland. Stress hormones can induce cellular senescence in peripheral tissues through pathways involving p53, p21, p16, or SA-β-GAL.[44] Cortisol was recently reported to bind to the glucocorticoid receptor, directly stimulating p53, which subsequently activates the p21 pathway, resulting in cell cycle inhibition.[44,45] Interestingly, previous studies have shown that aged alopecia DPCs exhibit increased p16 expression compared with non-alopecia DPCs, indicating that environmental stress and stress-induced senescence are associated with elevated oxidative stress and DNA damage.[46] Furthermore, premature senescence

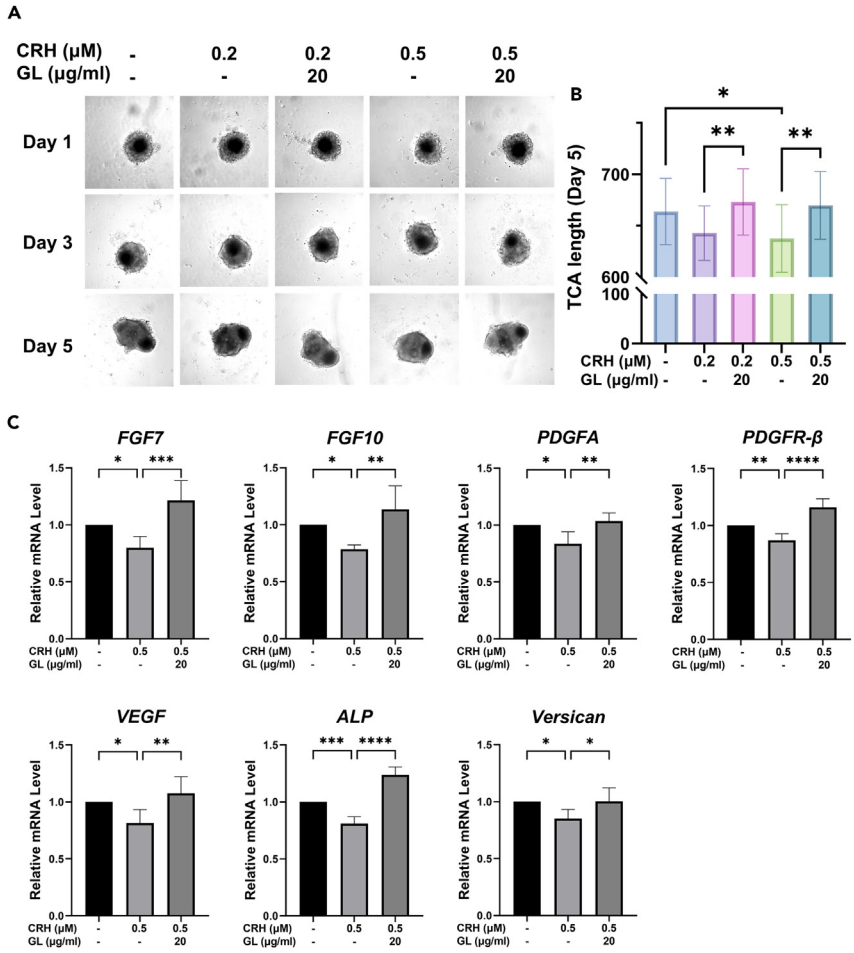

Figure 5. *Ganoderma lucidum* (GL) extract treatment blocks the inhibitory effects of corticotropin-releasing hormone (CRH) on hair growth

Two-cell assemblages (TCAs) were treated with CRH (0.2 μM–0.5 μM) in the absence or presence of GL extract (20 μg/mL) for 5 days.

(A) Representative images and (B) graph showing TCA length measured using high-content screening (HCS). The graph shows quantification results.

(C) The dermal papilla cells (DPCs) were treated with CRH (0.5 μM) in the absence or presence of GL extract (20 μg/mL) for 48 h. After 48 h, the cultured cells were harvested, and lysates were prepared for RT-qPCR. RT-qPCR analysis was performed to evaluate the expression levels of *FGF7*, *FGF10*, *PDGFA*, *PDGFR-β*, *VEGF*, *versican*, and *ALP* mRNAs. The graphs show the quantification results. ALP enzyme activity was analyzed by ALP staining (Figure S6A), and the quantification of hair follicle matrix cell proliferation was an assessed through Ki67 staining (Figure S6B). Data are presented as mean ± SD of five independent experiments. Statistical significance was calculated using one-way analysis of variance with Tukey's multiple comparisons test. *$p < 0.05$, **$p < 0.01$, ***$p < 0.001$, ****$p < 0.0001$.

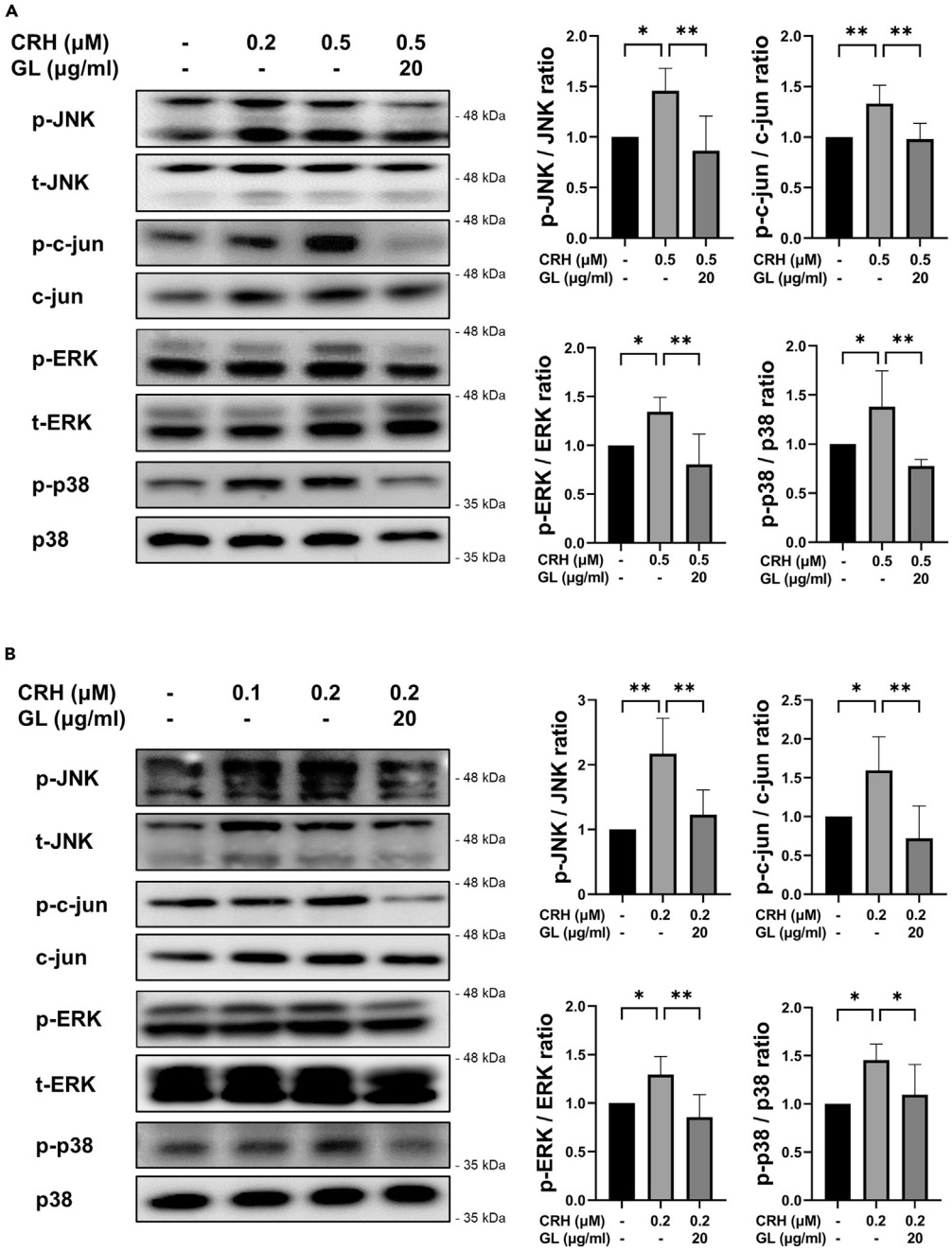

Figure 6. *Ganoderma lucidum* (GL) extract treatment prevents the phosphorylation of proteins in the MAPK signaling pathways in corticotropin-releasing hormone (CRH)-related stress response

(A) Dermal papilla cells (DPCs) and (B) outer root sheath cells (ORSCs) were treated with CRH (0.1 μM–0.5 μM) in the absence and the presence of GL extract (20 μg/mL) for 48 h. Cultured cells were harvested and western blotting was performed using antibodies against phospho-JNK, total-JNK, phospho-c-jun, total-c-jun, phospho-Erk1/2, total-Erk1/2, phospho-p38, and total-p38. Equal protein loading was confirmed based on total-JNK, total-c-jun, total-Erk1/2, and total-p38 levels. The graphs represent the quantification of the *p*-JNK/t-JNK, p-c-jun/c-jun, *p*-Erk1/2/t-Erk1/2, and p-p38/t-p38 protein expression. Data are presented as mean ± SD of five independent experiments. Statistical significance was calculated using one-way analysis of variance with Tukey's multiple comparisons test. *$p < 0.05$, **$p < 0.01$.

induced by stress hormones is associated with ROS production.[47] Moreover, *CRHR1* expression is upregulated in aged hair follicles, suggesting a systemic HPA stress response associated with aging.[21] In this study, we demonstrated that CRH induced cellular senescence via the activation of p53, p21, p16, or the SA-β-GAL marker, with the increased expression of Bax, suggesting that increased ROS production through

CRH mediates apoptosis. Conversely, the GL extract is known to exhibit antioxidant effects and possesses anti-aging properties, which increase longevity and inhibit ROS generation within cells.[31] Numerous studies have demonstrated that the bioactive components of GL eliminate hydroxyl radicals, 2,2-diphenyl-1-picrylhydrazyl (DPPH) radical activity, and lipid peroxidation, all of which contribute to potential ROS scavenging, reduced oxidative stress, and anti-aging effects against UVB-induced photoaging.[34] Our results indicate that CRH treatment increased ROS production in both cell types. In contrast, the GL extract treatment reduced ROS formation in both cell types, thereby, reducing CRH-induced oxidative stress and exerting anti-cellular senescence effects. These results reveal that the GL extract affects stress-induced hair follicle senescence, underscoring its ability for ROS scavenging in hair follicle cells.

Elevated ROS levels activate a cascade of cellular stress signaling pathways, including the MAPK pathway, which encompasses extracellular signal-regulated kinases (ERKs), c-Jun N-terminal kinase (JNK), and p38.[48,49] Bonfiglio et al. suggested that the stress response is related to the MAPK signaling pathway triggered by CRH through CRHR1.[50,51] This activated signaling pathway is involved in elevated apoptosis due to stress, subsequently increasing cellular senescence in hair follicles.[52] We found that CRH treatment increased the phosphorylation of JNK, c-jun, Erk1/2, and p38 in both cell types. In contrast, the GL extract treatment reduced the phosphorylation of JNK, c-jun, Erk1/2, and p38 in the CRH-treated cells, indicating the attenuation of stress-induced responses. Thus, our findings suggest that the GL extract decreases CRH-induced cellular stress and attenuates stress-induced hair follicular senescence, possibly through its ROS-scavenging effects in hHFCs.

Several growth factors and cytokines can promote hair cell proliferation and stimulate hair cell regeneration, ultimately inducing the anagen stage of the hair cycle.[53] These effects could prevent hair loss and facilitate hair cell regeneration. For instance, PDGFA and PDGFR-β are highly expressed in DPCs during the anagen phase, playing an important role in hair growth.[54,55] ALP and versican are specific markers of DPCs and are highly expressed during the anagen phase.[56,57] FGF-7 and FGF-10 contribute to hair cell proliferation and regeneration.[58,59] Moreover, VEGF is an essential paracrine factor that promotes hair growth.[60] Given the pivotal role of DPCs in hair follicle growth signaling pathways, we examined the expression of genes associated with anagen induction in DPCs. In cultured cells, CRH decreased the gene expression of several growth factors and anagen-related markers, including *FGF-7*, *FGF-10*, *PDGFA*, *PDGFR-β*, *VEGF, ALP*, and *versican*. However, the GL extract treatment restored the expression of all these growth factors.

CRHR1 and CRHR2 were reported to be differentially expressed in human hair follicular cells.[14,25] Interestingly, in another study, a natural antagonist of the CRH receptor reversed the downregulation of ALP and anagen-related cytokines and blocked the activation of MAPK signaling by CRH.[61] In our study, CRH treatment increased the expression of CRHR1 and CRHR2 in hHFCs. These results are in agreement with those of previous studies on the expression of CRH-stimulated CRH receptors.[18,19] To further elucidate the mechanism of GL action, we investigated how GL acts on CRH-induced CRH receptors in human follicular cells. The expression of CRHR1 and CRHR2 was decreased by the CRHR1 antagonist (antalarmin) or the CRHR2 antagonist (astressin$_2$-B) with CRH in both cells (Figure S7). In addition, in the presence of CRH, the induction of CRH receptor expression by GL was reduced in human ORSCs and DPCs (Figure S7). These results suggest that the GL extract could acts as a CRHR antagonist causing the antagonization of the CRHR1 and CRHR2. Further studies on CRH-R antagonist effects of GL in human follicular cells are required for a better understanding of the underlying mechanism.

In conclusion, we investigated the effect of GL extract on CRH-induced cellular senescence, ROS production, ALP activity, and TCA elongation. The GL extract decreased cellular senescence by SA-β-GAL activities and reduced CRH-induced ROS in hair follicle cells. Moreover, the GL extract recovered the TCA elongation suppressed by CRH. Our findings demonstrate that the GL extract attenuates stress-induced follicular senescence via ROS scavenging, suggesting that it may be a potential candidate for addressing stress-induced hair loss.

Limitations of the study

This study had several limitations. First, the effects of GL extract on hair follicular senescence induced by CRH were validated using hHFCs, a 3D co-culture platform, and an *ex vivo* system, which have certain limitations. Second, we did not confirm through western blotting that GL activates the hair growth pathway. Lastly, the mechanism of GL-induced recovery of TCA elongation in the presence of CRH was not confirmed using 3D co-culture spheroids.

STAR★METHODS

Detailed methods are provided in the online version of this paper and include the following:

- KEY RESOURCES TABLE
- RESOURCE AVAILABILITY
  - Lead contact
  - Materials availability
  - Data and code availability
- METHOD DETAILS
  - Ethics statement
  - Experimental model and study participant details
  - Preparation of human dermal papilla and outer root sheath cells
  - Cell viability assay
  - Senescence-associated β-galactosidase assay
  - Real-time quantitative reverse transcription PCR (RT-qPCR)

SUPPLEMENTAL INFORMATION

Supplemental information can be found online at https://doi.org/10.1016/j.isci.2024.109675.

ACKNOWLEDGMENTS

This study was supported by the COSMAX BTI Research Fund (grant no. 0681-20220054).

AUTHOR CONTRIBUTIONS

Conceptualization, S.L., S.K., S.L., S.J., and T.S.H.; investigation, S.L., S.K., S.L., and S.J.; writing – original draft, S.L. and S.K; writing review & editing, S.L., S.K., S.L., and O.K.; resources, Y.K. and J.C.; supervision, O.K.

DECLARATION OF INTERESTS

The authors declare no competing interests.

Received: October 10, 2023
Revised: March 15, 2024
Accepted: April 3, 2024
Published: April 6, 2024

REFERENCES

1. Tumbar, T., Guasch, G., Greco, V., Blanpain, C., Lowry, W.E., Rendl, M., and Fuchs, E. (2004). Defining the epithelial stem cell niche in skin. Science *303*, 359–363. https://doi.org/10.1126/science.1092436.
2. Paus, R., and Cotsarelis, G. (1999). The biology of hair follicles. N. Engl. J. Med. *341*, 491–497. https://doi.org/10.1056/NEJM199908123410706.
3. Matsumura, H., Mohri, Y., Binh, N.T., Morinaga, H., Fukuda, M., Ito, M., Kurata, S., Hoeijmakers, J., and Nishimura, E.K. (2016). Hair follicle aging is driven by transepidermal elimination of stem cells via COL17A1 proteolysis. Science *351*, aad4395. https://doi.org/10.1126/science.aad4395.
4. Gokce, N., Basgoz, N., Kenanoglu, S., Akalin, H., Ozkul, Y., Ergoren, M.C., Beccari, T., Bertelli, M., and Dundar, M. (2022). An overview of the genetic aspects of hair loss and its connection with nutrition. J. Prev. Med. Hyg. *63*, E228–E238. https://doi.org/10.15167/2421-4248/jpmh2022.63.2S3.2765.
5. Alexopoulos, A., and Chrousos, G.P. (2016). Stress-related skin disorders. Rev. Endocr. Metab. Disord. *17*, 295–304. https://doi.org/10.1007/s11154-016-9367-y.
6. Pacák, K., and Palkovits, M. (2001). Stressor specificity of central neuroendocrine responses: implications for stress-related disorders. Endocr. Rev. *22*, 502–548. https://doi.org/10.1210/edrv.22.4.0436.
7. Arck, P.C., Slominski, A., Theoharides, T.C., Peters, E.M.J., and Paus, R. (2006). Neuroimmunology of stress: skin takes center stage. J. Invest. Dermatol. *126*, 1697–1704. https://doi.org/10.1038/sj.jid.5700104.
8. Slominski, A., and Wortsman, J. (2000). Neuroendocrinology of the skin. Endocr. Rev. *21*, 457–487. https://doi.org/10.1210/edrv.21.5.0410.
9. Slominski, A., Wortsman, J., Luger, T., Paus, R., and Solomon, S. (2000). Corticotropin releasing hormone and proopiomelanocortin involvement in the cutaneous response to stress. Physiol. Rev. *80*, 979–1020. https://doi.org/10.1152/physrev.2000.80.3.979.
10. Slominski, A.T., Slominski, R.M., Raman, C., Chen, J.Y., Athar, M., and Elmets, C. (2022). Neuroendocrine signaling in the skin with a special focus on the epidermal neuropeptides. Am. J. Physiol. Cell Physiol. *323*, C1757–C1776. https://doi.org/10.1152/ajpcell.00147.2022.
11. Paus, R., Botchkarev, V.A., Botchkareva, N.V., Mecklenburg, L., Luger, T., and Slominski, A. (1999). The skin POMC system (SPS). Leads and lessons from the hair follicle. Ann. N. Y. Acad. Sci. *885*, 350–363. https://doi.org/10.1111/j.1749-6632.1999.tb08690.x.
12. Paus, R., Peters, E.M., Eichmüller, S., and Botchkarev, V.A. (1997). Neural mechanisms of hair growth control. J. Invest. Dermatol. Symp. Proc. *2*, 61–68. https://doi.org/10.1038/jidsymp.1997.13.
13. Ito, N., Ito, T., Kromminga, A., Bettermann, A., Takigawa, M., Kees, F., Straub, R.H., and Paus, R. (2005). Human hair follicles display a functional equivalent of the hypothalamic-pituitary-adrenal axis and synthesize cortisol. Faseb. J. *19*, 1332–1334. https://doi.org/10.1096/fj.04-1968fje.
14. Slominski, A.T., Zmijewski, M.A., Zbytek, B., Tobin, D.J., Theoharides, T.C., and Rivier, J. (2013). Key role of CRF in the skin stress response system. Endocr. Rev. *34*, 827–884. https://doi.org/10.1210/er.2012-1092.
15. Skobowiat, C., Dowdy, J.C., Sayre, R.M., Tuckey, R.C., and Slominski, A. (2011). Cutaneous hypothalamic-pituitary-adrenal axis homolog: regulation by ultraviolet radiation. Am. J. Physiol. Endocrinol. Metab. *301*, E484–E493. https://doi.org/10.1152/ajpendo.00217.2011.
16. Slominski, A., Zbytek, B., Semak, I., Sweatman, T., and Wortsman, J. (2005). CRH stimulates POMC activity and corticosterone production in dermal fibroblasts. J. Neuroimmunol. *162*, 97–102. https://doi.org/10.1016/j.jneuroim.2005.01.014.
17. Slominski, A., Zbytek, B., Szczesniewski, A., Semak, I., Kaminski, J., Sweatman, T., and Wortsman, J. (2005). CRH stimulation of corticosteroids production in melanocytes is mediated by ACTH. Am. J. Physiol. Endocrinol. Metab. *288*, E701–E706. https://doi.org/10.1152/ajpendo.00519.2004.
18. Lee, E.Y., Nam, Y.J., Kang, S., Choi, E.J., Han, I., Kim, J., Kim, D.H., An, J.H., Lee, S., Lee, M.H., and Chung, J.H. (2020). The local hypothalamic-pituitary-adrenal axis in cultured human dermal papilla cells. BMC

Mol. Cell Biol. *21*, 42. https://doi.org/10.1186/s12860-020-00287-w.

19. Fischer, T.W., Bergmann, A., Kruse, N., Kleszczynski, K., Skobowiat, C., Slominski, A.T., and Paus, R. (2021). New effects of caffeine on corticotropin-releasing hormone (CRH)-induced stress along the intrafollicular classical hypothalamic-pituitary-adrenal (HPA) axis (CRH-R1/2, IP(3) -R, ACTH, MC-R2) and the neurogenic non-HPA axis (substance P, p75(NTR) and TrkA) in ex vivo human male androgenetic scalp hair follicles. Br. J. Dermatol. *184*, 96–110. https://doi.org/10.1111/bjd.19115.
20. Botchkarev, V.A. (2003). Stress and the hair follicle: exploring the connections. Am. J. Pathol. *162*, 709–712. https://doi.org/10.1016/S0002-9440(10)63866-7.
21. Elewa, R.M., Abdallah, M., Youssef, N., and Zouboulis, C.C. (2012). Aging-related changes in cutaneous corticotropin-releasing hormone system reflect a defective neuroendocrine-stress response in aging. Rejuvenation Res. *15*, 366–373. https://doi.org/10.1089/rej.2011.1294.
22. Roloff, B., Fechner, K., Slominski, A., Furkert, J., Botchkarev, V.A., Bulfone-Paus, S., Zipper, J., Krause, E., and Paus, R. (1998). Hair cycle-dependent expression of corticotropin-releasing factor (CRF) and CRF receptors in murine skin. Faseb. J. *12*, 287–297. https://doi.org/10.1096/fasebj.12.3.287.
23. Botchkarev, V.A., Botchkareva, N.V., Slominski, A., Roloff, B., Luger, T., and Paus, R. (1999). Developmentally regulated expression of alpha-MSH and MC-1 receptor in C57BL/6 mouse skin suggests functions beyond pigmentation. Ann. N. Y. Acad. Sci. *885*, 433–439. https://doi.org/10.1111/j.1749-6632.1999.tb08706.x.
24. Slominski, A., Wortsman, J., Pisarchik, A., Zbytek, B., Linton, E.A., Mazurkiewicz, J.E., and Wei, E.T. (2001). Cutaneous expression of corticotropin-releasing hormone (CRH), urocortin, and CRH receptors. Faseb. J. *15*, 1678–1693. https://doi.org/10.1096/fj.00-0850rev.
25. Slominski, A., Pisarchik, A., Tobin, D.J., Mazurkiewicz, J.E., and Wortsman, J. (2004). Differential expression of a cutaneous corticotropin-releasing hormone system. Endocrinology *145*, 941–950. https://doi.org/10.1210/en.2003-0851.
26. Choi, S.J., Cho, A.R., Jo, S.J., Hwang, S.T., Kim, K.H., and Kwon, O.S. (2013). Effects of glucocorticoid on human dermal papilla cells *in vitro*. J. Steroid Biochem. Mol. Biol. *135*, 24–29. https://doi.org/10.1016/j.jsbmb.2012.11.009.
27. Choi, S., Zhang, B., Ma, S., Gonzalez-Celeiro, M., Stein, D., Jin, X., Kim, S.T., Kang, Y.L., Besnard, A., Rezza, A., et al. (2021). Corticosterone inhibits GAS6 to govern hair follicle stem-cell quiescence. Nature *592*, 428–432. https://doi.org/10.1038/s41586-021-03417-2.
28. Hu, F., Yan, Y., Wang, C.W., Liu, Y., Wang, J.J., Zhou, F., Zeng, Q.H., Zhou, X., Chen, J., Wang, A.J., and Zhou, J.D. (2019). Article Effect and Mechanism of Ganoderma lucidum Polysaccharides on Human Fibroblasts and Skin Wound Healing in Mice. Chin. J. Integr. Med. *25*, 203–209. https://doi.org/10.1007/s11655-018-3060-9.
29. Xu, Z., Chen, X., Zhong, Z., Chen, L., and Wang, Y. (2011). Ganoderma lucidum polysaccharides: immunomodulation and potential anti-tumor activities. Am. J. Chin. Med. *39*, 15–27. https://doi.org/10.1142/S0192415X11008610.
30. Shi, M., Zhang, Z., and Yang, Y. (2013). Antioxidant and immunoregulatory activity of Ganoderma lucidum polysaccharide (GLP). Carbohydr. Polym. *95*, 200–206. https://doi.org/10.1016/j.carbpol.2013.02.081.
31. Wang, J., Cao, B., Zhao, H., and Feng, J. (2017). Emerging Roles of Ganoderma Lucidum in Anti-Aging. Aging Dis. *8*, 691–707. https://doi.org/10.14336/AD.2017.0410.
32. Hsu, C.L., and Yen, G.C. (2014). Ganoderic Acid and Lucidenic Acid (Triterpenoid). Enzymes *36*, 33–56. https://doi.org/10.1016/B978-0-12-802215-3.00003-3.
33. Zhonghui, Z., Xiaowei, Z., and Fang, F. (2014). Ganoderma lucidum polysaccharides supplementation attenuates exercise-induced oxidative stress in skeletal muscle of mice. Saudi J. Biol. Sci. *21*, 119–123. https://doi.org/10.1016/j.sjbs.2013.04.004.
34. Zeng, Q., Zhou, F., Lei, L., Chen, J., Lu, J., Zhou, J., Cao, K., Gao, L., Xia, F., Ding, S., et al. (2017). Ganoderma lucidum polysaccharides protect fibroblasts against UVB-induced photoaging. Mol. Med. Rep. *15*, 111–116. https://doi.org/10.3892/mmr.2016.6026.
35. Schieber, M., and Chandel, N.S. (2014). ROS function in redox signaling and oxidative stress. Curr. Biol. *24*, R453–R462. https://doi.org/10.1016/j.cub.2014.03.034.
36. Jang, S., Ohn, J., Kang, B.M., Park, M., Kim, K.H., and Kwon, O. (2020). "Two-Cell Assemblage" Assay: A Simple *in vitro* Method for Screening Hair Growth-Promoting Compounds. Front. Cell Dev. Biol. *8*, 581528. https://doi.org/10.3389/fcell.2020.581528.
37. Deussing, J.M., and Chen, A. (2018). The Corticotropin-Releasing Factor Family: Physiology of the Stress Response. Physiol. Rev. *98*, 2225–2286. https://doi.org/10.1152/physrev.00042.2017.
38. Pan, Y., and Lin, Z. (2019). Anti-aging Effect of Ganoderma (Lingzhi) with Health and Fitness. Adv. Exp. Med. Biol. *1182*, 299–309. https://doi.org/10.1007/978-981-32-9421-9_13.
39. Kauser, S., Slominski, A., Wei, E.T., and Tobin, D.J. (2006). Modulation of the human hair follicle pigmentary unit by corticotropin-releasing hormone and urocortin peptides. Faseb. J. *20*, 882–895. https://doi.org/10.1096/fj.05-5257com.
40. Stenn, K.S., Paus, R., Dutton, T., and Sarba, B. (1993). Glucocorticoid effect on hair growth initiation: a reconsideration. Skin Pharmacol. *6*, 125–134. https://doi.org/10.1159/000211097.
41. Paus, R., Handjiski, B., Czarnetzki, B.M., and Eichmüller, S. (1994). A murine model for inducing and manipulating hair follicle regression (catagen): effects of dexamethasone and cyclosporin A. J. Invest. Dermatol. *103*, 143–147. https://doi.org/10.1111/1523-1747.ep12392542.
42. Wang, W., Ji, P., and Dow, K.E. (2003). Corticotropin-releasing hormone induces proliferation and TNF-alpha release in cultured rat microglia via MAP kinase signalling pathways. J. Neurochem. *84*, 189–195. https://doi.org/10.1046/j.1471-4159.2003.01544.x.
43. Knapp, D.J., Whitman, B.A., Wills, T.A., Angel, R.A., Overstreet, D.H., Criswell, H.E., Ming, Z., and Breese, G.R. (2011). Cytokine involvement in stress may depend on corticotrophin releasing factor to sensitize ethanol withdrawal anxiety. Brain Behav. Immun. *25* (*Suppl 1*), S146–S154. https://doi.org/10.1016/j.bbi.2011.02.018.
44. Gao, X., Li, F., Liu, B., Wang, Y., Wang, Y., and Zhou, H. (2021). Cellular Senescence in Adrenocortical Biology and Its Disorders. Cells *10*, 3474. https://doi.org/10.3390/cells10123474.
45. Beauséjour, C.M., Krtolica, A., Galimi, F., Narita, M., Lowe, S.W., Yaswen, P., and Campisi, J. (2003). Reversal of human cellular senescence: roles of the p53 and p16 pathways. EMBO J. *22*, 4212–4222. https://doi.org/10.1093/emboj/cdg417.
46. Bahta, A.W., Farjo, N., Farjo, B., and Philpott, M.P. (2008). Premature senescence of balding dermal papilla cells *in vitro* is associated with p16(INK4a) expression. J. Invest. Dermatol. *128*, 1088–1094. https://doi.org/10.1038/sj.jid.5701147.
47. Gougoura, S., Liakos, P., and Koukoulis, G.N. (2010). Effect of CRH on NO bioavailability, ROS production and antioxidant defense systems in endothelial EAhy926 cells. Free Radic. Res. *44*, 803–812. https://doi.org/10.3109/10715762.2010.485988.
48. Son, Y., Cheong, Y.K., Kim, N.H., Chung, H.T., Kang, D.G., and Pae, H.O. (2011). Mitogen-Activated Protein Kinases and Reactive Oxygen Species: How Can ROS Activate MAPK Pathways? J. Signal Transduct. *2011*, 792639. https://doi.org/10.1155/2011/792639.
49. Obata, T., Brown, G.E., and Yaffe, M.B. (2000). MAP kinase pathways activated by stress: the p38 MAPK pathway. Crit. Care Med. *28*, N67–N77. https://doi.org/10.1097/00003246-200004001-00008.
50. Bonfiglio, J.J., Inda, C., Refojo, D., Holsboer, F., Arzt, E., and Silberstein, S. (2011). The corticotropin-releasing hormone network and the hypothalamic-pituitary-adrenal axis: molecular and cellular mechanisms involved. Neuroendocrinology *94*, 12–20. https://doi.org/10.1159/000328226.
51. Nam, Y.J., Lee, E.Y., Choi, E.J., Kang, S., Kim, J., Choi, Y.S., Kim, D.H., An, J.H., Han, I., Lee, S., et al. (2020). CRH receptor antagonists from Pulsatilla chinensis prevent CRH-induced premature catagen transition in human hair follicles. J. Cosmet. Dermatol. *19*, 3058–3066. https://doi.org/10.1111/jocd.13328.
52. Yang, Y.C., Fu, H.C., Wu, C.Y., Wei, K.T., Huang, K.E., and Kang, H.Y. (2013). Androgen receptor accelerates premature senescence of human dermal papilla cells in association with DNA damage. PLoS One *8*, e79434. https://doi.org/10.1371/journal.pone.0079434.
53. Nanney, L.B., Stoscheck, C.M., King, L.E., Jr., Underwood, R.A., and Holbrook, K.A. (1990). Immunolocalization of epidermal growth factor receptors in normal developing human skin. J. Invest. Dermatol. *94*, 742–748. https://doi.org/10.1111/1523-1747.ep12874601.
54. Tomita, Y., Akiyama, M., and Shimizu, H. (2006). PDGF isoforms induce and maintain anagen phase of murine hair follicles. J. Dermatol. Sci. *43*, 105–115. https://doi.org/10.1016/j.jdermsci.2006.03.012.
55. Kamp, H., Geilen, C.C., Sommer, C., and Blume-Peytavi, U. (2003). Regulation of PDGF and PDGF receptor in cultured dermal papilla cells and follicular keratinocytes of the human hair follicle. Exp. Dermatol. *12*, 662–672. https://doi.org/10.1034/j.1600-0625.2003.00089.x.

56. Yamauchi, K., and Kurosaka, A. (2009). Inhibition of glycogen synthase kinase-3 enhances the expression of alkaline phosphatase and insulin-like growth factor-1 in human primary dermal papilla cell culture and maintains mouse hair bulbs in organ culture. Arch. Dermatol. Res. *301*, 357–365. https://doi.org/10.1007/s00403-009-0929-7.

57. Soma, T., Tajima, M., and Kishimoto, J. (2005). Hair cycle-specific expression of versican in human hair follicles. J. Dermatol. Sci. *39*, 147–154. https://doi.org/10.1016/j.jdermsci.2005.03.010.

58. Iino, M., Ehama, R., Nakazawa, Y., Iwabuchi, T., Ogo, M., Tajima, M., and Arase, S. (2007). Adenosine stimulates fibroblast growth factor-7 gene expression via adenosine A2b receptor signaling in dermal papilla cells. J. Invest. Dermatol. *127*, 1318–1325. https://doi.org/10.1038/sj.jid.5700728.

59. Lin, W.H., Xiang, L.J., Shi, H.X., Zhang, J., Jiang, L.P., Cai, P.T., Lin, Z.L., Lin, B.B., Huang, Y., Zhang, H.L., et al. (2015). Fibroblast growth factors stimulate hair growth through beta-catenin and Shh expression in C57BL/6 mice. BioMed Res. Int. *2015*, 730139. https://doi.org/10.1155/2015/730139.

60. Lachgar, S., Moukadiri, H., Jonca, F., Charveron, M., Bouhaddioui, N., Gall, Y., Bonafe, J.L., and Plouët, J. (1996). Vascular endothelial growth factor is an autocrine growth factor for hair dermal papilla cells. J. Invest. Dermatol. *106*, 17–23. https://doi.org/10.1111/1523-1747.ep12326964.

61. Nam, Y.J., Lee, E.Y., Choi, E.J., Kang, S., Kim, J., Choi, Y.S., Kim, D.H., An, J.H., Han, I., Lee, S., et al. (2020). CRH receptor antagonists from prevent CRH-induced premature catagen transition in human hair follicles. J. Cosmet. Dermatol. *19*, 3058–3066. https://doi.org/10.1111/jocd.13328.

STAR★METHODS

KEY RESOURCES TABLE

REAGENT or RESOURCE	SOURCE	IDENTIFIER
Antibodies		
Rabbit monoclonal anti-p16 INK4A (D3W8G) antibody, unconjugated	Cell Signaling Technology	Cat #92803, RRID: AB_2750891
Rabbit monoclonal anti-p21 Waf1/Cip1 (12D1) antibody, unconjugated	Cell Signaling Technology	Cat #2947, RRID: AB_823586
Rabbit polyclonal anti-Bax antibody, unconjugated	Cell Signaling Technology	Cat #2772, RRID: AB_10695870
Rabbit polyclonal anti-phospho-c-jun (ser73) antibody, unconjugated	Cell Signaling Technology	Cat #9164, RRID: AB_330892
Rabbit polyclonal anti-c-jun antibody, unconjugated	Cell Signaling Technology	Cat # 9165, RRID: AB_2130165
Rabbit polyclonal anti-phospho-SAPK/JNK (Thr183/Tyr185) antibody, unconjugated	Cell Signaling Technology	Cat #9251, RRID: AB_331659
Rabbit polyclonal anti-SAPK/JNK antibody, unconjugated	Cell Signaling Technology	Cat #9252, RRID: AB_2250373
Rabbit polyclonal anti-phospho-p44/42 MAPK (Erk1/2) (Thr202/Tyr204) antibody, unconjugated	Cell Signaling Technology	Cat #9101, RRID: AB_331646
Rabbit polyclonal anti-p44/42 MAPK (Erk1/2) antibody, unconjugated	Cell Signaling Technology	Cat #9102, RRID: AB_330744
Rabbit polyclonal anti-phospho-p38 MAPK (Thr180/Tyr182) antibody, unconjugated	Cell Signaling Technology	Cat #9211, RRID: AB_331641
Rabbit polyclonal anti-p38 MAPK antibody, unconjugated	Cell Signaling Technology	Cat #9212, RRID: AB_330713
Goat polyclonal CRF1/CRHR1 antibody, unconjugated	Abcam	Cat #ab77686, RRID: AB_1566096
Rabbit polyclonal CRHR2 antibody, unconjugated	Abcam	Cat #ab236982
Anti-beta actin antibody	Invitrogen	Cat #MA5-15739, RRID: AB_10979409
Mouse monoclonal anti-Human Ki-67 antigen, Clone MIB-1, unconjugated	Dako	Cat #M7240, RRID: AB_2142367
Goat anti-mouse IgG secondary antibody, Alexa Fluor™ 488	Invitrogen	Cat #A11001, RRID: AB_2534069
Rabbit anti-goat IgG secondary antibody, Alexa Fluor™ 594	Invitrogen	Cat #A11080, RRID: AB_2534124
Goat anti-rabbit IgG secondary antibody, Alexa Fluor™ 594	Invitrogen	Cat #A11012, RRID: AB_141359
Goat anti-rabbit IgG antibody	Genetex	Cat #GTX213110-01, RRID: AB_10618573
Donkey anti-goat IgG antibody	Genetex	Cat #GTX232040-01, RRID: AB_2887583
Goat anti-mouse IgG antibody	Genetex	Cat #GTX213111-01, RRID: AB_10618076
Chemicals, peptides, and recombinant proteins		
Corticotropin-releasing hormone	Sigma-Aldrich	Cat #05230050
Antalarmin hydrochloride	Tocris	Cat #2778
Astressin$_2$-B	Tocris	Cat #2391
Cell counting Kit-8	Dojindo	Cat #CK04
Senescence beta-galactosidase staining kit	Cell Signaling Technology	Cat #9860S
2′,7′-dichlorodihydrofluorescein diacetate (DCF-DA)	Sigma-Aldrich	Cat #D6883
NBT/BCIP stock solution	Sigma-Aldrich	Cat #11681451001
Mytomycin C	Sellekchem	Cat #S8146_50μg
L-glutamine	Gibco	Cat #25030-081
Insulin solution from bovine pancreas	Sigma-Aldrich	Cat #10516
Sodium pyruvate	Gibco	Cat #11360-070
MEM NEAA	Gibco	Cat #11140-050
Hydrocortisone	Sigma-Aldrich	Cat #H0135
Bovine serum albumin	EMD Millipore	Cat #126593
Protein quantification kit-BCA	Biomax	Cat #BCA0500

(*Continued on next page*)

Continued

REAGENT or RESOURCE	SOURCE	IDENTIFIER
RIPA buffer	Intronbio	Cat #IBS-BR002
Protease inhibitor cocktail tablets	Roche	Cat #70021000
Phosphatase inhibitor cocktail 2	Sigma-Aldrich	Cat #P5726
ECL Femto	Dyne Bio	Cat #GBE-F100
Triton X-100 solution	Sigma-Aldrich	Cat #X100
4′,6-Diamidino-2-phenylindole, dilactate (DAPI)	BioLegend	Cat #422801
Dimethyl sulfoxide (DMSO)	Sigma-Aldrich	Cat #D2650
Fetal bovine serum (FBS)	Thermo Fisher Scientific	Cat #16000-044
Phosphate-buffered saline (PBS)	Thermo Fisher Scientific	Cat #70-013-032
Protein Block Serum-free	Dako	Cat #X0909
Human Growth Factor Antibody Array C1	RayBiotech	Cat #AAG-GF-1
Experimental models: Cell lines		
Human male donor 01: adult dermal papilla_donor-01	This study	hDP-01
Human male donor 02: adult dermal papilla_donor-02	This study	hDP-02
Human male donor 03: adult dermal papilla_donor-03	This study	hDP-03
Human male donor 01: adult dermal papilla_donor-04	This study	hDP-04
Human female donor 05: adult dermal papilla_donor-05	This study	hDP-05
Human male donor 01: adult outer root sheath_donor-01	This study	hORS-01
Human male donor 02: adult outer root sheath_donor-02	This study	hORS-02
Human male donor 03: adult outer root sheath_donor-03	This study	hORS-03
Human male donor 01: adult outer root sheath_donor-04	This study	hORS-04
Human female donor 05: adult outer root sheath_donor-05	This study	hORS-05
Oligonucleotides		
Primer for *GAPDH* Forward: GTCTCCTCTGACTTCAACAGCG	This paper	N/A
Primer for *GAPDH* Reverse: ACCACCCTGTTGCTGTAGCCAA	This paper	N/A
Primer for *p16* Forward: CTCGTGCTGATGCTACTGAGGA	This paper	N/A
Primer for *p16* Reverse: GGTCGGCGCAGTTGGGCTCC	This paper	N/A
Primer for *p21* Forward: AGGTGGACCTGGAGACTCTCAG	This paper	N/A
Primer for *p21* Reverse: TCCTCTTGGAGAAGATCAGCCG	This paper	N/A
Primer for *p53* Forward: CCTCAGCATCTTATCCGAGTGG	This paper	N/A
Primer for *p53* Reverse: TGGATGGTGGTACAGTCAGAGC	This paper	N/A
Primer for *IL-6* Forward: AGACAGCCACTCACCTCTTCAG	This paper	N/A
Primer for *IL-6* Reverse: TTCTGCCAGTGCCTCTTTGCTG	This paper	N/A
Primer for *FGF7* Forward: CTGTCGAACACAGTGGTACCTG	This paper	N/A
Primer for *FGF7* Reverse: CCAACTGCCACTGTCCTGATTTC	This paper	N/A
Primer for *FGF10* Forward: TGAGAAGAACGGGAAGGTCAGC	This paper	N/A
Primer for *FGF10* Reverse: TGGCTTTGACGGCAACAACTCC	This paper	N/A
Primer for *PDGFA* Forward: GCCCATTCGGAGGAAGAG	This paper	N/A
Primer for *PDGFA* Reverse: TTGGCCACCTTGACGCTGCG	This paper	N/A
Primer for *PDGFR-β* Forward: CAGCTCTGGCCCTCAAAGG	This paper	N/A
Primer for *PDGFR-β* Reverse: AGCAGGTCAGAACGAAGGTG	This paper	N/A
Primer for *VEGF* Forward: TTGCCTTGCTGCTCTACCTCCA	This paper	N/A
Primer for *VEGF* Reverse: GATGGCAGTAGCTGCGCTGATA	This paper	N/A
Primer for *Alp* Forward: GCTGTAAGGACATCGCCTACCA	This paper	N/A
Primer for *Alp* Reverse: CCTGGCTTTCTCGTCACTCTCA	This paper	N/A

(*Continued on next page*)

Continued

REAGENT or RESOURCE	SOURCE	IDENTIFIER
Primer for *versican* Forward: TGTGGCCCAAAATGGAAATA	This paper	N/A
Primer for *versican* Reverse: GTGTGTACCTGCTGGTTGCC	This paper	N/A
Software and algorithms		
GraphPad Prism 9.5	GraphPad	https://www.graphpad.com/scientific-software/prism/ RRID:SCR_002798
ImageJ/FIJI	National Institutes of Health	https://imagej.nih.gov/ij/, https://imagej.net/Fiji RRID:SCR_003070

RESOURCE AVAILABILITY

Lead contact

Further information and requests for resources should be directed to the lead contact, Ohsang Kwon (oskwon@snu.ac.kr).

Materials availability

This study did not generate unique reagents.

Data and code availability

- All data reported in this paper will be shared by the lead contact upon request.
- This paper does not report original code.
- Any additional information required to reanalyze the data reported in this paper is available from the lead contact upon request.

METHOD DETAILS

Ethics statement

The studies involving human participants were reviewed and approved by the Institutional Review Board of Seoul National University (protocol number 1101-116-353). All the patients provided written consent to participate in this study.

Experimental model and study participant details

Human hair follicles were obtained from the scalp skin tissue of four adult male donors and one adult female donor (key resources table) at Seoul National University Hospital, Seoul.

Preparation of human dermal papilla and outer root sheath cells

Candlelight-shaped human dermal papilla cells (DPCs) were dissected and isolated from single hair follicles using a no. 20 blade and a 1 ml syringe needle under a stereomicroscope. Subsequently, these cells were cultured in Dulbecco's modified Eagle's medium (DMEM; Welgene) supplemented with 20% fetal bovine serum (FBS; Welgene) and antibiotic/antimycotic (penicillin and streptomycin; Gibco). After a two-week incubation period, the DPCs were well-attached and the medium was changed to DMEM containing 10% FBS. Outer root sheath cells (ORSCs) were isolated from the hair shaft and bulb and immersed in DMEM supplemented with 20% FBS. After the third or fourth day, the medium was replaced with KBMTM-2 Basal Medium (Lonza) supplemented with KGMTM-2 SingleQuotsTM Supplement Pack (Lonza) and antibiotic/antimycotic. All cells were incubated at 37°C in a humidified environment with 5% CO_2.[36]

Cell viability assay

DPCs and ORSCs were plated in triplicate in a 96-well plate at a density of 5×10^3 cells/well. DPCs and ORSCs were treated with CRH at concentrations of 0.2–1 μM and 0.1–0.5 μM, respectively, for 48 h at 37°C in a humidified atmosphere with 5% CO_2. Following treatment with CRH, cell viability was assessed using the Cell counting kit-8 (CCK-8; Dojindo). CCK-8 solution was added to each well according to the manufacturer's instructions. The absorbance was measured at 450 nm using a microplate reader (VersaMax, Molecular Device Corporation), and cell viability was calculated relative to that in the DMSO control (Figure S1).

Senescence-associated β-galactosidase assay

To measure premature senescence induced by CRH, DPCs and ORSCs were seeded in 6-well plates at a density of 5×10^4 cells/well. The DPCs and ORSCs were treated with 0.2–0.5 μM and 0.1–0.2 μM CRH, respectively, for 48 h. To assess the inhibitory effects of GL extract on senescence, DPCs and ORSCs were treated with 0.5 and 0.2 μM CRH, respectively, for 24 h and subsequently incubated with CRH in the absence or presence of GL extract (20 μg/ml) for an additional 24 h. *Ganoderma lucidum* extract (Ganoxyl™; Lot. HJ-220511L) was

purchased from COSMAX BTI. The senescence-associated β-galactosidase (SA-β-GAL) assay was conducted using the senescence β-galactosidase staining kit (Cell Signaling Technology), according to the manufacturer's instructions. Cells were stained overnight at 37°C and subsequently imaged under a bright field microscope (Nikon). Cell counting was performed using ImageJ/FIJI (NIH).

Real-time quantitative reverse transcription PCR (RT-qPCR)

Total RNA was isolated using RNA iso Plus (TaKaRa Bio) following the manufacturer's instructions. One microgram of total RNA was used for cDNA synthesis using a Revert Aid First Strand cDNA Synthesis kit (Thermo Fisher), according to the manufacturer's instructions. qPCR was performed using a 7500 Real-Time PCR System (Applied Biosystems) and SYBR green Master Mix (Bioneer) according to the manufacturer's instructions. The expression of each gene was normalized to that of *GAPDH*. The relative mRNA expression levels were calculated based on the mRNA levels of the control (Figure S2), using the comparative threshold cycle (ΔΔCt) method on the 7500 Real-Time PCR System. All experiments were performed in triplicate and independently repeated four times. The primer sequences used in this study are listed in the key resources table.

Western blot analysis

Cells were lysed in RIPA protein extraction solution (BD Bio-sciences) containing protease (Roche) and phosphatase (Sigma-Aldrich) inhibitors. Total protein was separated on 10% and 15% sodium dodecyl sulfate-polyacrylamide gel electrophoresis (SDS-PAGE) gels and transferred onto polyvinylidene (PVDF) membranes (Millipore) using Tris-Glycine buffer. Membranes were blocked with 5% skim milk in TBS + 0.1% Tween-20 and incubated overnight at 4°C with the following primary antibodies (Cell Signally Technology): anti-p16 (1:500 dilution), anti-p21 (1:1000 dilution), anti-Bax (1:1000 dilution), anti-phospho-JNK (1:500 dilution), anti-JNK (1:1000 dilution), anti-phospho-c-jun (1:500 dilution), anti-c-jun (1:1000 dilution), anti-phospho-Erk1/2 (1:1000 dilution), anti-Erk1/2 (1:1000 dilution), anti-phospho-p38 (1:1000 dilution), and anti-p38 (1:1000 dilution). Anti-β-actin antibody (1:2000 dilution; Invitrogen) was used as a control. After incubation with the primary antibodies, the membranes were incubated with goat anti-rabbit or goat anti-mouse horseradish peroxidase conjugated secondary antibodies (GeneTex) for 1 h at 25°C. Blots were detected using an electrochemiluminescence (ECL) assay. Signals were detected using the ECL Plus Western blotting detection system (Amersham Imager 680, GE). Quantitative densitometry of protein bands was performed using the ImageJ software.

Two-cell assemblage assay

Cultured DPCs (passages 1–3; 3×10^3 cells/well) were seeded in round-bottom ultra-low attachment 96-well plates (Costar) in DMEM. The cells aggregated into spherical structures after 5 days of incubation. Subsequently, we added cultured ORSCs (passage 1 or 2; 5×10^3 cells/well) into each well, replacing the medium with Willam's E Medium (Gibco) supplemented with 2 mM L-glutamine (Gibco), 10 ng/ml hydrocortisone (Sigma), and 10 μg/ml insulin (Sigma).[36] To determine the effect of CRH on the length of the 3D co-cultured DPCs and ORSCs (two-cell assemblage, TCA), they were treated with CRH at various concentrations (0.2–0.5 μM) for 5 days. The length of the TCA was subsequently measured. To determine the effects of GL extract on the length of the TCA, the cells were treated with CRH at various concentrations (0.2–0.5 μM) for 2 days, and then with the GL extract (20 μg/ml) in combination with CRH for 3 days. The recovery length was subsequently measured. Throughout the experimental period (from days 1–5), the culture medium was supplemented with designated concentrations of CRH and GL. The length of the TCA was measured using a high-content imaging system (HCS, Image Xpress, Molecular Devices).

Human growth factor antibody array

DPCs were seeded, and upon reaching 100% confluency, they were treated with the GL extract (20 μg/ml) in serum-free KGM-Gold™ keratinocyte growth medium (Lonza). Thereafter, the conditioned medium was collected, and the filtrate was subsequently centrifuged using 3-kDa weight cut-off Vivaspin (Sartorius Stedim Biotech GmbH) to perform a growth factor array analysis. The analysis was conducted using the Human Growth Factor Antibody Array C1 (RayBiotech) following the manufacturer's instructions.

Alkaline phosphatase activity

DPCs were seeded in 6-well plates at a density of 5×10^4 cells/well. The cells were then treated with CRH (0.2–0.5 μM) or GL extract (20 μg/ml) in combination with CRH for 48 h at 37°C in a humidified atmosphere with 5% CO_2. Subsequently, the cells were fixed in 4% paraformaldehyde for 10 min at 25°C and washed with PBS. The cells were then rinsed in TN buffer (0.1 M Tris-HCl, 0.15 M NaCl, and 1 mM $MgCl_2$) and subsequently incubated in a solution containing 120 μg/ml 4-nitroblue tetrazolium and 60 μg/ml BCIP (5-brono-4-chloro-3-indolyphophate) in TN buffer for 25 min at 37°C in a humidified atmosphere with 5% CO_2. The reaction was terminated by washing with PBS containing 20 mM EDTA. ALP-positive cells were visualized under a bright field microscope (Nikon) and counted using the ImageJ/FIJI software (NIH).

H_2DCF-DA fluorescence intensity in cells

Fluorescence intensity was determined using 2,7-dichlorodihydrofluorescein diacetate (H2DCF-DA; Invitrogen). To measure CRH-induced ROS formation, DPCs and ORSCs were seeded in 6-well plates at a density of 5×10^4 cells/well. The DPCs and ORSCs were treated with 0.2–0.5 μM and 0.1–0.2 μM CRH, respectively, for 48 h at 37°C in a humidified atmosphere with 5% CO_2. To assess the effects of ROS scavenging by the GL extract, DPCs and ORSCs were initially treated with 0.5 and 0.2 μM CRH, respectively, for 24 h. Subsequently, the cells were

incubated with CRH in the presence or absence of the GL extract (20 μg/ml) for an additional 24 h. Cells were treated with H_2O_2 (200 μM) as a positive control for 2 h at 37°C. After treatment, the cells were washed twice with PBS and incubated with 20 μM DCF-DA in PBS for 30 min at 37°C in a humidified atmosphere with 5% CO_2. After incubation, the cells were washed twice with PBS. Nuclei were counterstained with 4′,6-diamidino-2-phenylindol (DAPI, 1:1000, Invitrogen) for 1 min. The cells were washed again with PBS, and cytoplasm DCF-DA and nuclear DAPI staining was imaged using an inverted fluorescence microscope (Leica).

Quantitative determination of ROS

Quantitative analysis of cellular ROS levels was conducted using H2DCF-DA. Both cell types were seeded in 96-well plates at a density of 5×10^3 cells/well. After washing the cells with PBS, they were incubated in PBS containing 20 μM H_2DCF-DA and 1% FBS for 30 min at 37°C in a humidified atmosphere with 5% CO_2. After washing with PBS, the absorbance of H_2DCF-DA was measured using an ELISA reader (Tecan, Spark) at 535 nm following excitation at 485 nm. For flow cytometry analysis (FACS Canto II, BD), we conducted experiments involving individual concentrations of CRH treatment followed by treatment with the GL extract to evaluate ROS scavenging induced by CRH. Additionally, we verified the general ROS scavenging effect of the GL extract compared with that in the DMSO treatment. For positive control, H_2O_2 (200 μM) was applied before H_2DCF-DA treatment. After these steps, the cells were incubated with H_2DCF-DA for 30 min at 37°C.

Immunofluorescence analysis

For Ki67 staining, anagen hair follicles were isolated through micro-dissection and surrounding adipose tissue and sebaceous glands were trimmed with a no. 20 blade under a stereomicroscope (Olympus). These hair follicles were then incubated in 12-well plates in the presence of 0.5 μM CRH or 0.5 μM CRH with 20 μg/ml GL extract in William's E medium (Gibco) for 48 h. Hair follicles were mounted on Tissue-Tek cryo-OCT compound (Epredia) and frozen on dry ice. The frozen blocks were sectioned at a thickness of 10 μm at −25°C. The tissue was incubated with mouse monoclonal anti-human Ki67 (DAKO) at a 1:100 dilution overnight at 4°C. Secondary goat anti-mouse antibodies labeled with Alexa Flour 488 (Invitrogen) were applied and incubated for 1 h at 25°C. Nuclei were stained with DAPI (1:1000). The number of Ki67-positive cells relative to the total number of DPAI-positive cells was determined. Ki67 and nuclear DAPI were imaged using an upright microscope (Nikon), and cell counting was performed using the ImageJ/FIJI software (NIH).

Corticosterone releasing hormone receptor antagonist treatment and immunocytochemistry

After seeding, DPCs (4×10^3 cells/well) and ORSCs (8×10^3 cells/well) were incubated with CRH in the absence or presence of the GL extract (20 μg /ml) for 24 h at 37°C. CRH-R antagonists were added 1 h before CRH treatments. Antalarmin (1 μM), a selective CRH-R1 antagonist (Tocris), and astressin$_2$-B (1 μM), a CRH-R2 antagonist (Tocris), were used (Figures S7A and S7C). For CRH-R1/2 staining, cells were fixed in 4% paraformaldehyde for 20 min 25°C and washed with PBS. Subsequently, blocking was performed with serum-free protein block (Dako) for 10 min. The cells were incubated with anti-CRH-R1 (1:100, dilution) and anti-CRH-R2 (1:100, dilution) overnight at 4°C. Thereafter, the cells were incubated with secondary antibodies, rabbit anti-goat and goat anti-rabbit labeled with Alexa Flour 594 (Invitrogen) for 1 h at 25°C. Nuclei were stained with DAPI (1:1000) for 30 min. All images were obtained using confocal microscopy (STELLARIS 5, Leica). The fluorescence of CRHR1 (green) and CRHR2 (red) staining, excluding the DAP-stained nuclei, was normalized based on the fluorescence threshold for the control group (Figures S7B and S7D). This normalization was performed consistently using the ImageJ/FIJI software (NIH).

QUANTIFICATION AND STATISTICAL ANALYSIS

Statistics and reproducibility

Statistical analyses were performed using GraphPad Prism (GraphPad Software Inc., version 9.5). Data are represented as the mean ± standard deviation (SD). Differences between results were assessed using the unpaired Student's *t*-test and one-way analysis of variance (ANOVA) followed by Dunnett's T3 test and Tukey's multiple comparisons test for significance. In all statistical comparisons, $*p < 0.05$, $**p < 0.01$, $***p < 0.001$, and $****p < 0.0001$ were considered to indicate significant differences.